

## Detection of inplane and outofplane ultrasonic displacements by a twochannel confocal Fabry–Perot interferometer

A. Cand, J.P. Monchalin, and X. Jia

Citation: *Applied Physics Letters* **64**, 414 (1994); doi: 10.1063/1.111141

View online: <http://dx.doi.org/10.1063/1.111141>

View Table of Contents: <http://scitation.aip.org/content/aip/journal/apl/64/4?ver=pdfcov>

Published by the [AIP Publishing](#)

---

### Articles you may be interested in

#### [EMAT MEASUREMENTS OF IN AND OUTFPLANE ULTRASONIC SIGNALS](#)

*AIP Conf. Proc.* **975**, 841 (2008); 10.1063/1.2902751

#### [In-plane and out-of-plane band-gap properties of a two-dimensional triangular polymer-based void channel photonic crystal](#)

*Appl. Phys. Lett.* **84**, 4415 (2004); 10.1063/1.1758298

#### [Micromachined Fabry–Perot interferometer for motion detection](#)

*Appl. Phys. Lett.* **81**, 3320 (2002); 10.1063/1.1518557

#### [Simultaneous measurements of inplane and outofplane surface displacements of shell vibrations at several points by an array of miniature laser probe heads](#)

*J. Acoust. Soc. Am.* **93**, 2389 (1993); 10.1121/1.406041

#### [Optical detection of ultrasound at a distance using a confocal Fabry–Perot interferometer](#)

*Appl. Phys. Lett.* **47**, 14 (1985); 10.1063/1.96411

---



**physicstoday**

Comment on any  
*Physics Today* article.

Physics Today / Volume 65 / Issue 1 / January 2012  
Previous Article | Next Article  
**Measured energy in Japan**  
David von Seggern  
(dovon@seismo.uni-erlangen.de) University of  
July 2012, page 10  
DIGITAL OBJECT IDENTIFIER  
<http://dx.doi.org/10.1063/PT.3.1619>  
The article by Thorne Lay and Hiroo Kanamori  
to a 100-megaton explosion...  
this is not right. If the authors would...  
relationship between seismic moment...  
ment, they would find that the...  
released a 100-megaton nuclear...  
times as much energy: a...  
100-megaton at

...while that of a 100-megaton...  
approximately five times as much energy...  
nuclear detonation event...  
The 1964 Chilean earthquake had still more energy by a factor of about 3, or 10 times...  
release. The seismic energy underestimate the total strain energy release by a variable that depends on friction...  
on the fault plane. Accounting for total strain energy release would increase the earthquake energy number by...  
orders of magnitude.  
Despite the catastrophic damage potential of nuclear bombs, the forces of nature occasionally unleash much...  
larger energy releases. Although the nuclear bombs are under our control, earthquakes, volcanic eruptions, and...  
extreme weather events are not. However, by judicious preparation and avoidance measures, humans can...  
significantly diminish the damage of natural events.  
This article does not have any references.

**Comment on this article**  
By the act of hitting a ball with a bat, one calculates the force energy to deliver the ball to its new...  
location, but one must also take into account that the ball extended its energy release to that...  
which became struck by the ball as its momentum ceased and passed energy to the struck team...  
Therefore the parameters of the damage extend into the future when the received energy to that...  
pushed upon, later becomes released in a new event. Perhaps calculations of one added that in...  
while another's calculations did not. E.M.C.  
Written by Edgar McCarville, 14 July 2012 19:59

# Detection of in-plane and out-of-plane ultrasonic displacements by a two-channel confocal Fabry–Perot interferometer

A. Cand and J.-P. Monchalín

National Research Council Canada, Industrial Materials Institute, 75 De Mortagne Boulevard, Boucherville, Québec J4B 6Y4, Canada

X. Jia

Groupe de Physique des Solides, Université Paris 7, 2 place Jussieu, Tour 23, 75251 Paris Cedex 05, France

(Received 22 March 1993; accepted for publication 9 November 1993)

Simultaneous detection of in-plane and out-of-plane ultrasonic displacements by a two-channel confocal Fabry–Perot optical receiver is described. Accuracy is tested by measuring the in-plane and out-of-plane displacements produced by Rayleigh surface waves generated by a piezoelectric transducer and a laser.

Generation and detection of ultrasonic waves by lasers has been recognized to present numerous advantages for nondestructive inspection and characterization of materials.<sup>1,2</sup> This technique is particularly useful in cases where conventional piezoelectric-based techniques cannot be applied, e.g., in the case of specimens at elevated temperature or contoured specimens. Many of these contoured specimens used, e.g., in the aeronautic and automotive industries, are thin and made of a single sheet of metal or composite material or of multiple sheets bonded together. The use of ultrasonic plate waves has been considered for testing such specimens, either using piezoelectric generation<sup>3</sup> or more recently laser generation.<sup>4–6</sup> In the case of piezoelectric generation, the transducer is generally tilted with respect to the normal in a given plane, while in the case of laser generation, the laser is often focused along a small line. In both cases, the generated waves, which appear as a complex pattern of modes, propagate in a well-defined direction, so they have only two displacement components, one tangential (in-plane) in the direction of wave propagation and one perpendicular to the surface (out-of-plane). Better understanding of the mode pattern and of the effect on this pattern on bonding conditions and defects within the plate could be obtained if the two components can be separated by the optical detection probe. This is not usually possible, since the probe measures the displacement along its line of sight, which is in general a combination of the in-plane and out-of-plane displacements. In this letter, we describe a system which can measure separately and at the same time these two components. Although the detection and measurement of ultrasonic vector displacements have been previously considered<sup>2,7</sup> and the measurement of the in-plane and out-of-plane components have been demonstrated<sup>8–10</sup> by using a combination of optical heterodyning (reference interferometry)<sup>7</sup> and differential interferometry,<sup>7,11</sup> the systems developed so far are speckle sensitive and require precise focusing onto the surface, which make them, in practice, only suitable to laboratory experimentation. The system described in this letter is based instead on a confocal Fabry–Perot.<sup>12,13</sup> The confocal Fabry–Perot receiver is known to be speckle insensitive from the fact that the multiple delayed waves within the Fabry–Perot cavity have, in good approximation, the same distribution as

the incident wave scattered by the surface, even if this one is affected by thousands of speckles. A large number of speckles also means that precise focusing onto the surface is not required and, consequently, such a system is very suitable for use in industry.

Determination of the two components of the ultrasonic field at the surface of the sample is obtained by using two detection channels in a single confocal Fabry–Perot interferometer, as shown in Fig. 1. The surface is illuminated by a laser beam along its normal  $z$  and scattered light is collected symmetrically along two directions making an angle  $\Theta$  with  $z$ . For a given direction of detection, the phase shift caused by a surface displacement  $\delta(t)$  of components  $\delta x$  and  $\delta z$  is given by

$$\Psi = (\mathbf{k}_i - \mathbf{k}_s) \cdot \delta(t), \quad (1)$$

where  $\mathbf{k}_i$  is the incident light wave vector and  $\mathbf{k}_s$  is the wave vector of light scattered into one of the detection directions. Therefore, the phase variation of light received along channel 1 is equal to  $(2\pi/\lambda)(-\delta z - \delta z \cos \Theta + \delta x \sin \Theta)$ , whereas it is equal to  $(2\pi/\lambda)(-\delta z - \delta z \cos \Theta - \delta x \sin \Theta)$  for light received along channel 2,  $\lambda$  being the optical wavelength. As-

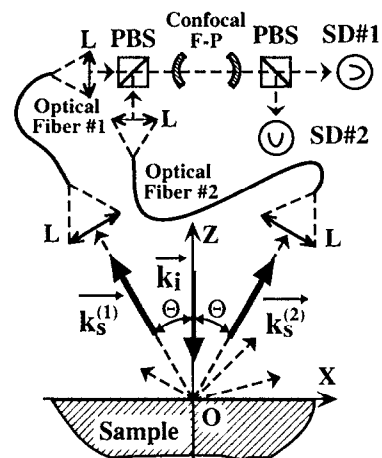


FIG. 1. Schematic of principle and of the optical setup. (L): lens, (PBS): polarizing beam splitter, (SD): signal detector, (F-P): Fabry–Perot interferometer.

suming further that the two channels have the same sensitivity (same collected light intensity, same interferometer response, same detector sensitivity) and harmonic ultrasonic displacement at frequency  $f_u[\delta x = u_x \cos(2\pi f_u t + \phi_x)$  and  $\delta z = u_z \cos(2\pi f_u t + \phi_z)]$ , we obtain after addition and subtraction of the output intensity signals  $I^{(1)}$  and  $I^{(2)}$  along the two channels

$$I^{(1)} + I^{(2)} = -I_0 \frac{4\pi}{\lambda} S_{FP}(f_u) u_z (1 + \cos \Theta) \times \cos[2\pi f_u t + \phi_{FP}(f_u) + \phi_z], \quad (2a)$$

$$I^{(1)} - I^{(2)} = I_0 \frac{4\pi}{\lambda} S_{FP}(f_u) u_x \sin \Theta \times \cos[2\pi f_u t + \phi_{FP}(f_u) + \phi_x], \quad (2b)$$

where  $I_0$  is the intensity transmitted by one channel for zero displacement and  $S_{FP}(f_u)$  and  $\phi_{FP}(f_u)$  are, respectively, the amplitude and the phase of the response of the phase discriminator constituted by the confocal Fabry–Perot for small ultrasonic displacements at frequency  $f_u$ .<sup>13</sup> These functions  $S_{FP}$  and  $\phi_{FP}$  are readily calculated by sending at the input of a confocal Fabry–Perot a light field at the laser frequency plus two fields at the optical sidebands frequencies, which are equal to the laser frequency  $\pm f_u$ , and by calculating the intensity at the output of the interferometer.<sup>13</sup> Therefore the sum is proportional to the normal (out-of-plane) component of the displacement and the difference to its tangential (in-plane) component. In the case of nonharmonic ultrasonic displacements, where the detection is linear for small ultrasonic displacements, the sum and difference of the intensity signals are expressed by the integrals over ultrasonic frequency of the left-hand side of Eqs. 2(a) and 2(b),  $u_x, \phi_x, u_z, \phi_z$  now being the amplitude and phase spectra of the displacement.

The optical configuration, which is also shown in Fig. 1, uses a cw argon ion laser ( $\lambda = 514.5$  nm) for illumination of the surface. The collection angle  $\Theta$  is  $31.3^\circ$  and the spot size on the surface is about  $50 \mu\text{m}$  obtained by focusing with a long focal lens. This spot size is smaller than the ultrasonic wavelengths to be considered in this work. Added flexibility is obtained by using two large core optical fibers to transmit collected light to the interferometer. The core diameter and the numerical aperture of the fibers are chosen to match the interferometer étendue or throughput.<sup>7,12</sup> The two detection channels are separated by means of polarizing beam splitters at the input of the interferometer and in front of the detectors, as shown in Fig. 1. For the work reported here where the ultrasonic signal is in the range 1–10 MHz, the confocal Fabry–Perot is used in the transmission mode. Note that operation in the reflection mode, which is known to increase sensitivity at higher ultrasonic frequencies,<sup>14</sup> could also have been used. The confocal Fabry–Perot used in this work is 50 cm long, has an optical bandwidth of  $\sim 9$  MHz, and is frequency stabilized to half-maximum transmission.<sup>12,13</sup> This bandwidth provides adequate sensitivity for the 1–10 MHz range,<sup>13</sup> and gives also an étendue adapted to the coupling fibers used. Avalanche photodiodes are used as detectors. Their outputs after bandpass filtering (0.5–20 MHz) are si-

multaneously digitally sampled by a two-channel data acquisition system and then transferred to a microcomputer for processing.

The performance of the technique was tested by measuring the in-plane and out-of-plane components of a Rayleigh surface wave, as done previously for the system based on optical heterodyning and differential interferometry.<sup>9</sup> Such a wave is known to be nondispersive and its components have well-known theoretical values, calculated for planar and curved surfaces.<sup>15</sup> For plane harmonic Rayleigh wave propagation on a planar surface, the theoretical ratio of out-of-plane to in-plane displacement components at the surface of a solid and their phase difference are given by the following equations:

$$\frac{u_z}{u_x} = \frac{\frac{C_R^2}{C_S^2} \sqrt{1 - \frac{C_R^2}{C_L^2}}}{2 - \frac{C_R^2}{C_S^2} - 2 \sqrt{1 - \frac{C_R^2}{C_L^2}} \sqrt{1 - \frac{C_R^2}{C_S^2}}}, \quad (3a)$$

$$\phi_z - \phi_x = \pi/2, \quad (3b)$$

where  $C_R, C_L$ , and  $C_S$  are the Rayleigh, longitudinal, and shear velocities, respectively. Using the values measured for an aluminum alloy sample used in this work ( $C_L = 6260$  m/s,  $C_S = 3170$  m/s,  $C_R = 2964$  m/s, Eq. (5) gives the theoretical ratio  $u_z/u_x = 1.565$ . As indicated by Eq. 3(b), theory also predicts also a phase lead of  $\pi/2$  of the out-of-plane component over the in-plane component. In practice, according to the direction of propagation of the surface wave, an additional phase shift equal to  $\pi$  may be introduced to the in-plane signal and one should expect to measure a phase difference of  $\pi/2$  between the two components.

The specimen used was an aluminum alloy bar of square cross section ( $\sim 1$  in.). The probed surface was gently scratched with sandpaper in one direction to enhance light scattering in the plane of the setup. Tests were performed with piezoelectric generation using a narrow-band ( $\sim 2.2$  MHz) piezoelectric transducer mounted on a wedge and laser generation. In the case of laser generation, strong signals were obtained by vaporizing a thin coating (paint) layer with a Q-switched Nd:YAG laser. The laser beam was focused onto the sample surface to a small line of approximately 10 mm long and less than 0.4 mm wide, perpendicular to the length of the bar. Such a line source is known to produce a Rayleigh surface wave with good directivity,<sup>16</sup> which propagates essentially in the direction perpendicular to the generation line, i.e., along the length of the bar. Detection was performed on axis of the line source at 10.5 mm from it. Light scattering from the surface of the bar was to some extent anisotropic and caused the intensities received by the two channels to be different, so the signals were normalized to the light intensities measured by the two detectors before adding and subtracting the signals from the two channels. The useful parts of both signals were windowed and then Fourier transformed. The ratio of their amplitudes and their phase difference was finally calculated and compared to theoretical predictions.

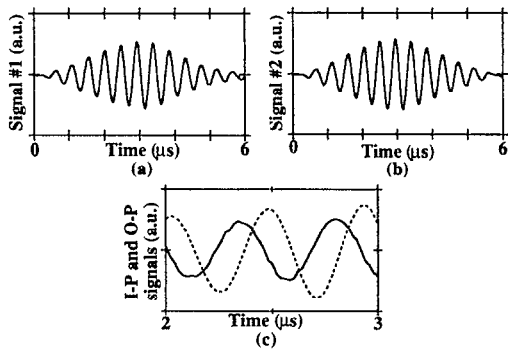


FIG. 2. Results obtained by surface wave generation with a piezoelectric transducer mounted on a wedge: (a) signal detected on channel No. 1, (b) signal detected on channel No. 2, (c) in-plane (solid line) and out-of-plane (dashed line) components of the surface motion.

Experimental results are shown in Fig. 2 for piezoelectric generation and in Fig. 3 for laser generation. Figures 2(a) and 2(b) show the signals detected directly along the two channels, when the piezoelectric transducer is excited by a pulsed oscillator providing a driving voltage similar to the signal observed optically. Figure 2(c) shows the in-plane (solid line) and out-of-plane (dashed line) signals calculated from the data of Figs. 2(a) and 2(b) on an expanded time scale. As expected, these two signals appear in quadrature. Detailed analysis shows that their phase shift is  $-103^\circ$ . The amplitude ratio is found equal to 1.737, off by 11% from the theoretical ratio. Departure from theory could be explained by inaccuracy in the evaluation of the angle  $\Theta$ , nonperfect symmetry of the setup, and a surface perturbation which is not exactly a Rayleigh surface wave, but includes perturbations caused by reflections from the side of the bar and within the launching wedge.

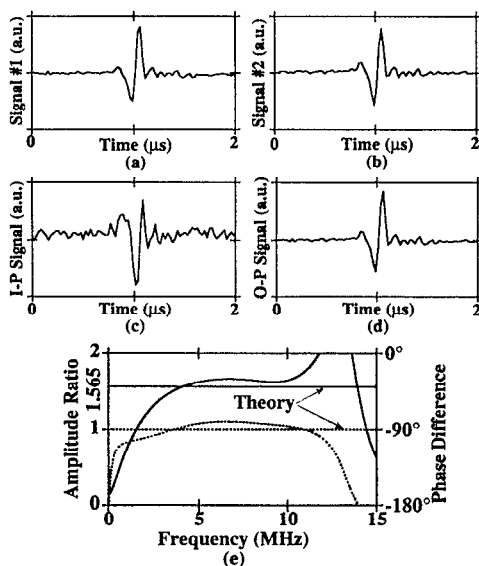


FIG. 3. Results obtained by laser generation: (a) signals detected on channel 1, (b) signal detected on channel 2, (c) in-plane component, (d) out-of-plane component, (e) ratio of the amplitudes (solid line) and phase difference (dashed line) vs ultrasonic frequency.

The single shot signals recorded on each channel in the case of laser generation are shown in Figs. 3(a) and 3(b). Figures 3(c) and 3(d) show the in-plane and out-of-plane signals calculated from the data of Figs. 3(a) and 3(b). The ratio of the amplitude spectra and the phase difference are plotted in Fig. 3(e) versus ultrasonic frequency. We observe a reasonable agreement in the 3–11 MHz range with the predicted theoretical values. The differences could be explained by some diffraction effect and by nonuniform generation across the line caused by the nonuniform intensity distribution of the laser beam. The diffraction effect is actually observed in the time domain by a trailing pulse after the main Rayleigh wave bipolar signal. Below 3 MHz and above 11 MHz, the amplitude and phase spectra are also inaccurate because of truncation and high-pass filtering. At high frequencies, accuracy also decreases because the diameter of the incident light spot becomes of the order of magnitude of the ultrasonic wavelength, making the pointlike detection approximation no longer valid.

In conclusion, we have shown that the two components of ultrasonic motion at the surface of an object can be detected simultaneously by using a two-channel confocal Fabry–Perot interferometer. This scheme can be used in industrial environments since it is not speckle sensitive and allows collection of light with multimode optical fibers. It could find some applications for testing with laser generated plate wave thin wall structures, either made of a single sheet of metal or composite material or of multiple sheets bonded together, which are common in the aeronautic and automotive industries. The ability to separate the in-plane motion from the out-of-plane motion could help to analyze the complex pattern of plate modes produced by laser impact and to interpret the effect of various flaws.

- <sup>1</sup>D. A. Hutchins, *Physical Acoustics*, edited by W. P. Mason and R. N. Thurston (Academic, New York, 1988), Vol. 18, pp. 21–123.
- <sup>2</sup>C. B. Scruby and L. E. Drain, *Laser-Ultrasonics: Techniques and Applications* (Hilger, Bristol, 1990), pp. 325–402.
- <sup>3</sup>G. M. Light and H. Kwun, *Nondestructive Evaluation of Adhesive Bond Quality: State-of-the-Art Review*, Nondestructive Testing Information Analysis Center (Southwest Research Institute, San Antonio, TX, 1989).
- <sup>4</sup>D. A. Hutchins, C. Saleh, M. Moles, and B. Farahbakhsh, *J. Nondestructive Eval.* **9**, 247 (1990).
- <sup>5</sup>A. C. Bushell, C. Edwards, S. B. Palmer, and H. Nakano, *Review of Progress in Quantitative NDE*, edited by D. O. Thompson and D. E. Chimenti (Plenum, New York, 1992), Vol. 11, p. 1315.
- <sup>6</sup>A. Cand, G. Quentin, and J.-P. Monchalain (unpublished).
- <sup>7</sup>J.-P. Monchalain, *IEEE Trans. Ultra. Ferroelectrics, Freq. Control UFFC-33*, 485 (1986).
- <sup>8</sup>R. Dandliker and J. F. Willemin, *Opt. Lett.* **6**, 165 (1981).
- <sup>9</sup>J.-P. Monchalain, J.-D. Aussel, R. Héon, C. K. Jen, A. Boudreault, and R. Bernier, *J. Nondestruct. Eval.* **8**, 121 (1989).
- <sup>10</sup>Probe available commercially from Ultra-Optec Inc, 27 de Lauzon, Boucherville, Qué, J4B 1E7, Canada, with trade name OP 35 I/O.
- <sup>11</sup>A. D. W. McKie and J. W. Wagner, *Appl. Phys. Lett.* **53**, 1043 (1988).
- <sup>12</sup>J.-P. Monchalain, *Appl. Phys. Lett.* **47**, 14 (1985).
- <sup>13</sup>J.-P. Monchalain and R. Héon, *Mater. Eval.* **44**, 1231 (1986).
- <sup>14</sup>J.-P. Monchalain, R. Héon, P. Bouchard, and C. Padioleau, *Appl. Phys. Lett.* **55**, 1612 (1989).
- <sup>15</sup>I. A. Viktorov, *Rayleigh and Lamb Waves* (Plenum, New York, 1967).
- <sup>16</sup>A. M. Aindow, R. J. Dewhurst, and S. B. Palmer, *Opt. Commun.* **42**, 116 (1982).